Fibroblast Growth Factor 4 Directs Gap Junction Expression in the Mesenchyme of the Vertebrate Limb Bud

H. Makarenkova, D.L. Becker, C. Tickle, and A.E. Warner

Department of Anatomy and Developmental Biology, University College London, London WC1E 6BT, United Kingdom

Abstract. Pattern in the developing limb depends on signaling by polarizing region mesenchyme cells, which are located at the posterior margin of the bud tip. Here we address the underlying cellular mechanisms. We show in the intact bud that connexin 43 (Cx43) and Cx32 gap junctions are at higher density between distal posterior mesenchyme cells at the tip of the bud than between either distal anterior or proximal mesenchyme cells. These gradients disappear when the apical ectodermal ridge (AER) is removed. Fibroblast growth factor 4 (FGF4) produced by posterior AER cells controls signaling by polarizing cells. We find that FGF4 doubles gap junction density and substantially improves functional coupling between cultured posterior mesenchyme cells. FGF4 has no effect on cultured anterior mesenchyme, suggesting that any effects of FGF4 on responding anterior mesenchyme cells are not mediated by a change in gap junction density or functional communication through gap junctions. In condensing mesenchyme cells, connexin expression is not affected by FGF4. We show that posterior mesenchyme cells maintained in FGF4 under conditions that increase functional coupling maintain polarizing activity at in vivo levels. Without FGF4, polarizing activity is reduced and the signaling mechanism changes. We conclude that FGF4 regulation of cell–cell communication and polarizing signaling are intimately connected.

PATTERNING of the skeleton in the vertebrate limb involves a number of cellular interactions. Antero–posterior patterning is controlled by the polarizing region (Saunders and Gasseling, 1968), a group of posterior mesenchyme cells near the tip of the limb bud that induce pattern duplication when transplanted to the anterior mesenchyme of a host limb bud. The signaling process is highly conserved because polarizing region cells can reprogram anterior mesenchyme across vertebrate species (e.g., Tickle et al., 1976). The tip of the limb bud mesenchyme is rimmed by the apical ectodermal ridge (AER).[1] When the ridge is removed, outgrowth and pattern formation within the limb bud ceases (Saunders, 1948; Summerbell, 1974).

Growth factor signaling plays a central role in limb bud patterning. Posterior apical ridge cells express fibroblast growth factor 4 (FGF4) transcripts, and FGF4 can maintain polarizing activity in the absence of the ridge (Niswander et al., 1993; Vogel and Tickle, 1993; Fallon et al., 1994). Cells in the polarizing region express *sonic hedgehog* gene transcripts, which are associated with polarizing activity (Riddle et al., 1993; Laufer et al., 1994). FGF4 drives *Shh* expression in the polarizing region (Laufer et al., 1994; Niswander et al., 1994); when the apical ridge is removed, *Shh* expression is reduced.

Growth factor signals in the developing limb may be linked to cell–cell interactions through gap junctions, which have been implicated in mediating cell patterning in the limb bud. Allen, Tickle, and Warner (1990) used antibodies to gap junction protein to interfere with communication through gap junctions; they showed that when communication between polarizing cells and anterior mesenchyme cells was prevented, duplication of the digits was substantially reduced. Green et al. (1994) noted a reduction in gap junction labeling at the tip of the limb bud when the AER was removed.

We need to understand the cellular mechanisms that contribute to limb bud signaling. This requires unraveling of both the hierarchy of the many signals now recognized to operate in the developing limb bud and the way in which they interact with each other. In this paper, we begin such a mechanistic analysis by testing the hypothesis that FGF4 controls the expression of gap junctions and functional communication in the mesenchyme.

Address all correspondence to Anne Warner, Department of Anatomy and Developmental Biology, University College London, Gower Street, London WC1E 6BT UK. Tel.: 171-380-7279. Fax: 171-419-3014. E-mail: a.warner@ucl.ac.uk

1. *Abbreviations used in this paper*: AER, apical ectodermal ridge; Cx, connexin; FGF, fibroblast growth factor; HH, Hamilton Hamburger.

Materials and Methods

Limb buds from chick (Hamilton Hamburger [HH] stages 20–21) or mouse (10.5–11 d) embryos were used. For studies of gap junction distribution in the intact bud, the limb bud was cut away at the base, embedded in optimal cutting temperature medium (OCT), oriented, frozen in isopentane cooled by liquid nitrogen, and mounted in OCT on chucks. Serial sections at 10 μm were taken through the entire limb bud. Sections were mounted on gelatinized slides. When quantitative comparisons were to be made between different regions of the limb bud, the bud was cut from posterior to anterior. Sections were stained with the appropriate antibodies or treated with propidium iodide to reveal the nuclei, as outlined below.

Micromass cultures were prepared as described in Vogel and Tickle (1993). Briefly, posterior and anterior regions were cut from the bud, and the ectoderm was removed after treatment with trypsin at 4°C. Material from either posterior or anterior regions of ~20 limb buds was pooled in 1 ml of medium (MEM + 10% FCS + antibiotics [GIBCO BRL, Paisley, UK]), dissociated by trituration with a yellow tip Eppendorf pipette, and then spun at 6,500 rpm in an Eppendorf centrifuge (Fremont, CA) for 2 min. The pellet was resuspended in culture medium (see below) to give a suspension of single cells. Cell density in a sample of the suspension was determined by counting in a haemocytometer, and suspensions were prepared at 4×10^4, 2×10^4, or 1×10^4 cells/10 μl. A 10-μl drop of cells at the chosen density was placed at the center of a small coverslip within each well of a four-well dish and left to attach for 20–25 min, and then 300 μl of culture medium was added. Chick mesenchyme cultures were maintained in F12/DME, 50/50 (GIBCO BRL), with 10% FCS (Sigma Chemical Co., Poole, UK) plus glutamine and antibiotic/antimycotic (GIBCO BRL). Mouse mesenchyme cultures were maintained in CMRL (GIBCO BRL) with FCS, glutamine, and antibiotic/antimycotic. The cultures were maintained for 24 h in an incubator at 37°C gassed with 5% CO_2 in air. When the effect of FGF4 was to be tested, it was added to the culture medium at 10 ng/ml. FGF4 was a kind gift of John Heath (University of Birmingham, UK). After 24 h, the cells had attached to the coverslip and spread to form a single culture about 5 mm in diameter. An example is shown in Fig. 3 *a*.

Immunocytochemistry

Frozen sections of chick or mouse limb bud, mounted on gelatinized slides, were washed in PBS for 10 min, blocked in 0.1 M L-lysine (Sigma Chemical Co.) in PBS, briefly washed in PBS, and stained with primary antipeptide, connexin-specific antibodies overnight at 4°C. After several washes in PBS, secondary antibody was applied for 1 h. Coverslips with attached micromass cultures were briefly washed in PBS, fixed in methanol for 2–5 min, washed in PBS, blocked and permeabilized in PBS with L-Lysine and Triton X-100 (Sigma Chemical Co.) 0.5%, and then stained with connexin-specific antibodies with the same schedule as frozen sections. The following polyclonal antibodies raised in rabbits were used (for characterizations see Becker et al., 1995): connexin 43 (Cx43): Gap 15 (amino acids [AA] 131–142), Gap 13 (AA 123–136); Cx32: Des 5 (AA 108–119), Des 1 (AA 102–112; 116–124); and Cx26: Des 3 (AA 106–119). The monoclonal antibody R521c (Developmental Biology Hybridoma Bank, Iowa State University) was used to recognize Cx32 in double labeling experiments. Primary antibodies were used at 1:50 or 1:100 dilution. Polyclonal primary antibodies were detected with swine anti–rabbit IgG conjugated to FITC (DAKO Corp., Denmark) and goat anti–rabbit IgG conjugated to Texas red (Molecular Probes, Eugene, OR). Monoclonal antibodies were detected with rabbit anti–mouse, rabbit anti–rat, or goat anti–mouse IgGs conjugated to FITC (DAKO Corp.) and Texas red (Molecular Probes) or to CY5 (BDS). Secondary antibodies were used at 1:30 dilution. For double staining, monoclonal and polyclonal antibodies were applied simultaneously and recognized with appropriate secondary antibodies. In some preparations, nuclei were stained by including dilute propidium iodide (0.001%) in one of the final washes. After staining, specimens were washed thoroughly in PBS, mounted in Citifluor, and examined on a laser scanning confocal microscope (model TCS4D; Leica, Inc., Milton Keynes, UK).

For all antibodies, the connexin specificity of staining was confirmed by: (*a*) omitting primary antibodies; (*b*) parallel staining of mouse heart (Cx43 only) and liver (Cx32, Cx26); and (*c*) peptide competition with the peptide used to raise the antibody, which was compared against competition with peptides other than the immunizing peptides. In all cases, the connexin specificity of the antibodies used was confirmed. Although chick Cx32 has not yet been sequenced, there is high homology between species in the cytoplasmic loop, the region from which peptides Des 1 and Des 5 were drawn. Western blots showed that Des 1 antibodies recognized a 32-kD protein in chick mesenchyme.

Confocal Microscopy and Quantitative Analysis

Sections or cultures were viewed on a Leica confocal microscope. 512 × 512–pixel images of single optical sections or projections through the depth of the culture were captured using a 63× objective and stored as digital images for quantitative analysis. Single optical sections were taken for analysis of undifferentiated regions of the cultures, and projections were used for analysis of condensations. Optical sections were collected 1 μm from the specimen surface to avoid surface contamination of the image. Projections were prepared from the same number of optical sections at 1-μm intervals throughout each culture, excluding the top 1 μm. Each projection through condensation aggregates was constructed from the same number of sections. To ensure consistency, images collected from the same experiment were prepared for analysis in the same session and all potential variables (pinhole, laser power, photomultiplier tube sensitivity) kept constant during image acquisition and between specimens.

Quantitative analysis was carried out as follows: A 60 × 60–μm-sided square (3,600 μm^2) was placed over the region to be analyzed. The region enclosed by the square was converted to a single image and imported into either PC Image (Foster Findlay Associates, Newcastle, UK) or NIH Image software for analysis (see Green et al., 1993). The threshold for creating a binary image for counting was kept constant between images and was set to ensure that spots that represented connexin labeling would be counted without interference from background; any blemishes that were clearly artifactual were removed from the image, and the number of spots above background was counted automatically. The minimum detectable plaque size was 0.1 μm^2, and there was no obvious change in the range or distribution of plaque sizes under the different conditions tested. Between 5 and 20 fields were analyzed for each set of measurements. The number of labeled gap junctions measured in each field was plotted as a frequency histogram; the mean, standard error of the mean, and median were calculated, and the distributions were compared using the nonparametric Mann–Whitney test. *P* values of less than 0.05 were considered to reflect a statistically significant difference.

For micromass cultures, samples were always taken from central regions of the culture because at the periphery cell, density began to decline. When analyzing intact limb buds, the limb bud was oriented so that the bud was cut from posterior to anterior. The first 20 and last 20 sections through the mesenchyme were used for quantitative analysis.

Tests of Polarizing Capacity

Micromass cultures were scraped off the dish and cut into 8–10 fragments of approximately equal size. Individual fragments were placed beneath the apical ectodermal ridge overlying the anterior mesenchyme of host chicks at stage 20. Anderson et al. (1993) showed that polarizing capacity was relatively insensitive to variations in fragment size; fragments that differed by a factor of two gave similar degrees of respecification. Host embryos were reincubated for a further 6 d, fixed in 5% TCA, and stained with alcian green to show the cartilage skeletal pattern. The digit pattern was scored to give a value for percentage respecification, as described in Allen et al. (1990). Limb duplications are scored according to the most posterior additional digit formed and sets an extra digit 2 only as 25% respecification, an extra digit 3 (in the presence or absence of digit 2) as 50% respecification, and likewise, an extra digit 4 as 100% respecification. The average, summed over all limb buds analyzed in each group, gives percentage respecification. (See Fig. 9 *a* for illustration of representative cartilage patterns after polarizing region grafts.)

Functional Analysis of Dye Transfer

Micromass cultures were plated at 1×10^4 cells/10 μl on small glass coverslips. At this density, the cells formed large islands rather than a complete monolayer and were well spread on the dish so that individual cell outlines were clearly visible. Injections were made into cells lying within one of the large islands to ensure that dye spread was not limited artificially by the number of cells available to receive dye. A coverslip containing a micromass culture was placed into the lid of a 35-mm Petri dish filled with serum-free culture medium on the stage of a fixed stage compound microscope (model M35; Micro Instruments, Oxford, UK) and viewed with either 10× or 40× long working distance (>6 mm) objectives. Omega dot Pyrex glass (Corning 7740; Glass Company of America) was pulled on a standard microelectrode puller to give micropipettes with a relatively short shank and tip diameters of less than 1 μm. The tip of the pipette was filled with 2% Lucifer yellow (Sigma Chemical Co.) in 100 mM NaCl, and a trail of fluid was left along the capillary to allow electrical contact with the half

cell. The pipette was held in an Ag/AgCl half cell on a Huxley micromanipulator (Johnson Matthey, London, UK) and connected to the input of a WPI amplifier (Clarke Electromedical, Pangbourne, UK); a second AgCl pellet was used to earth the bath. The pipette was inserted into the cell in voltage recording mode while viewed under a 40× objective, and the membrane potential was used to monitor the intracellular location of the pipette. Once a membrane potential had been recorded, a pulse of Lucifer yellow was ejected from the tip of the pipette by brief capacitative oscillation. The number of cells containing Lucifer yellow was counted, and transfer was assessed at intervals after injection. When dye spread was particularly efficient, dye dissipated into distant cells. The microscope was equipped with incident fluorescent light with appropriate filters for exciting and viewing Lucifer yellow during the injection. For cell counting and photography the objective was switched to a 40× (NA 0.4) objective (Nikon, Inc., London, UK). Photographs were taken with a Zeiss M35 camera (Welwyn Garden City, UK) on Kodak 400 film (Rochester, NY).

Results

A Gradient of Gap Junctions Is Present in the Chick Limb Bud

Gap junctions, detected by expression of Cx proteins, were not uniformly distributed in the limb bud. There were more labeled gap junctions in the posterior subapical mesenchyme, where polarizing cells are located, than in anterior regions. In proximal regions, the density of gap junctions declined and the posterior–anterior gradient disappeared.

Cx43 was widely expressed and present in gap junctions throughout the subapical mesenchyme and ridge ectoderm at the tip of the chick limb bud (Fig. 1 *a*). Mesenchyme cells, but not ridge ectoderm cells, expressed Cx32 protein also (Fig. 1 *b*). Connexin 26 was not detected. Almost all cells expressed both Cx43 and Cx32 (Fig. 1 *c*; Cx43 [*red*] and Cx32 [*green*]) in gap junctions. However, each connexin can be clearly distinguished, suggesting that Cx43 and Cx32 are not present in the same gap junction plaques. Mouse limb buds revealed a similar picture for Cx43 and 32 (see comparable sections in Fig. 1, *d–f*). Cx26 was detected in dorsal ectoderm (data not shown). These results are not the same as reported previously. Green et al. (1994) examined only Cx43 in chick limb buds, while Laird et al. (1992) found Cx43 restricted to the ectoderm, with only Cx32 in mouse mesenchyme. There is no obvious explanation for the differences; a combination of different preparative techniques and different antibodies is probably responsible.

The distribution of Cx43- and Cx32-labeled junctions across the chick limb bud was analyzed at HH stage 19–20 on single optical sections of frozen sections taken at posterior and anterior margins in both distal and proximal regions. The frequency distributions for Cx43-labeled gap junctions in posterior and anterior regions at the tip of the limb bud (up to 60 μm from the ridge ectoderm) are shown in Fig. 2, *a* and *c*, and show that there were 50–70% more gap junctions between cells in posterior regions. The distribution of Cx32-containing gap junctions at the tip of the limb bud revealed an equivalent gradient from posterior to anterior mesenchyme (posterior: median 46, range 38–65 gap junctions/3,600 μm^2; anterior: median 28, range 18–40 gap junctions/3,600 μm^2; posterior vs. anterior, $P < 0.003$).

The gap junction gradient was found only at the tip of the limb bud. In proximal regions (~150 μm back from the tip), there was no significant difference between posterior and anterior mesenchyme, and gap junction density was lower than at the tip (Cx43: Fig. 2, *b* and *d*). Cx32 showed the same decline and absence of posterior–anterior gradient in proximal regions.

Thus, there is a gradient of gap junction density across the limb bud, with polarizing region cells expressing significantly more gap junctions than other cells. Is this gradient controlled by the apical ectodermal ridge? 24 h after removal of the AER, the gradient between posterior and anterior mesenchyme gap junction density had completely disappeared (Cx43: posterior [556 ± 18.8 junctions per 3,600 μm^2] vs. anterior [525 ± 19 junctions per 3,600 μm^2] $P > 0.25$; three specimens), and at the tip, the average gap junction density was about half that found in normal limb buds. We conclude that the posterior–anterior gradient of gap junction density in the developing limb bud requires the presence of the AER.

FGF4 and Gap Junctions

Like gap junctions, transcripts for molecules such as *Shh* are asymmetrically distributed across the limb bud mesenchyme, with higher levels in the polarizing region. The asymmetric transcript distribution of *Shh* is dependent on secretion of FGF4 by posterior ridge ectoderm cells. Is the asymmetric distribution of Cx43- and Cx32-containing gap junctions in the mesenchyme also under the control of FGF4? Initially, we tested the consequences of applying FGF4 beads to intact limb buds lacking the AER, but quantitative analysis proved extremely difficult because the beads stapled to the outside of the bud interfered with the integrity of frozen sections. However, FGF4 can maintain polarizing activity of cultured mouse posterior mesenchyme cells (Vogel and Tickle, 1993). We therefore turned to micromass cultures of mesenchyme cells to test the hypothesis that FGF4 controls gap junctional communication.

Gap Junctions in Posterior Mesenchyme Are Dependent on FGF4

Gap junction density between posterior mesenchyme cells was exquisitely sensitive to FGF4. Fig. 3 illustrates Cx staining in chick and mouse cultures. Fig. 1, *j* and *k*, shows examples of Cx43 staining in chick posterior mesenchyme cultures in the absence (*j*) and presence (*k*) of FGF4. Figs. 4–6 show individual experiments drawn from the summed data given in Table I. A low power image of a chick limb bud culture stained for Cx43 (Fig. 3 *a*) shows the layer of undifferentiated mesenchyme, which includes small, scattered condensations. Undifferentiated cells between condensations expressed Cx43 around each cell (Fig. 3 *b*) and formed a monolayer (rotated image in Fig. 3 *c*). Cells in condensations expressed Cx43 (Fig. 3, *e* and *f*). In culture, chick cells expressed only Cx43 protein in gap junctions; Cx32 could not be detected, suggesting that Cx32 protein expression is reduced. Cultured mouse limb bud mesenchyme retained expression of both Cx32 and Cx43 (Fig. 3, *d*, *g*, and *h*). Antibody-stained junctions were counted either in condensations or in the monolayer (see Fig. 3 *a* and Materials and Methods).

Fig. 4 shows results from one of the experiments on chick limb bud mesenchyme and demonstrates the key ob-

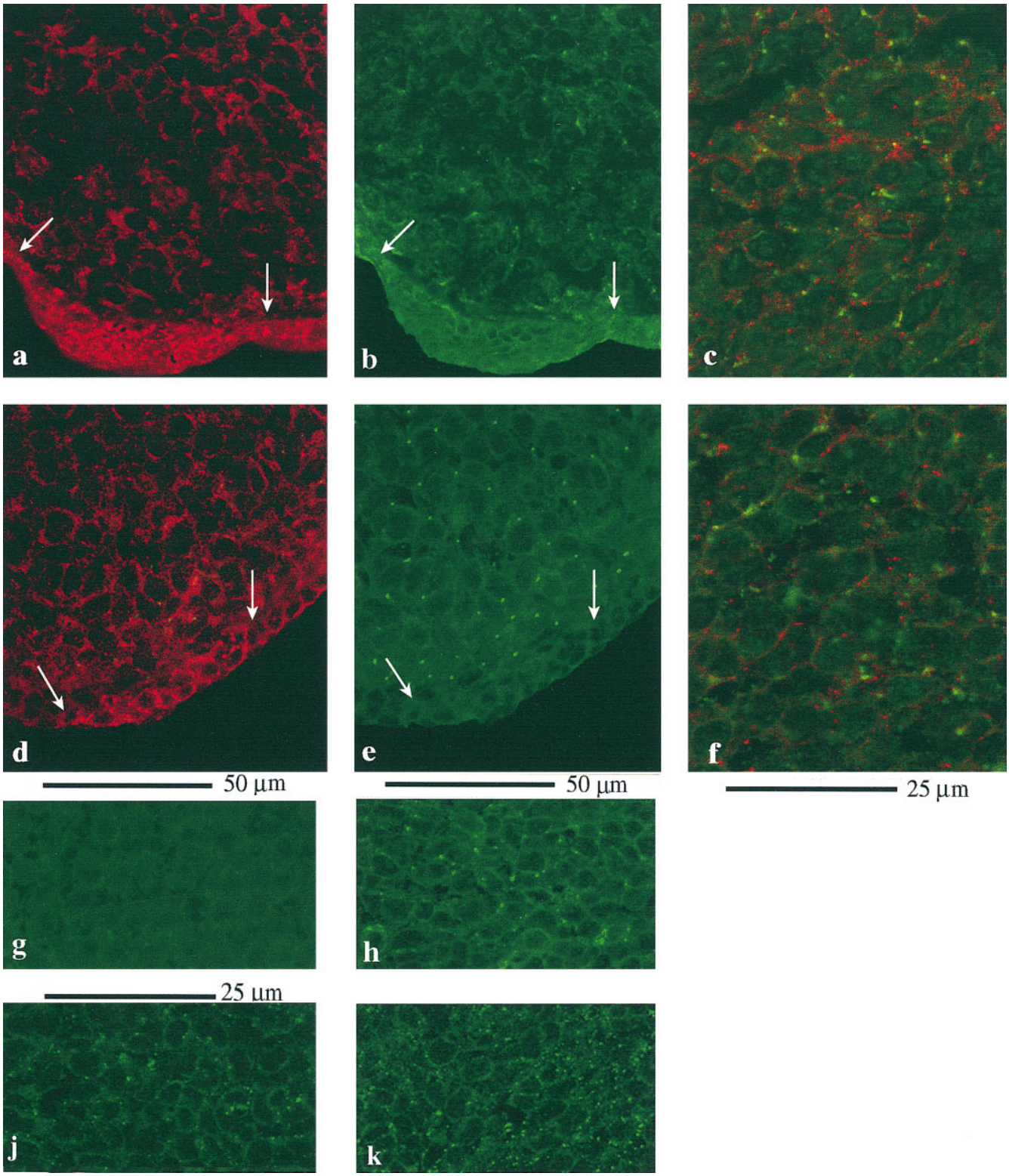

Figure 1. (*a–h*) Connexin staining in the intact limb bud. Sections through chick (*a–c*) and mouse (*d–h*) limb buds to show the pattern of gap junction protein expression. (*a*) Section through the tip of a chick limb bud stained for Cx43. Note dense expression of Cx43 between cells in the AER (between *arrows*). (*b*) Same section stained for Cx32. Occasional Cx32 gap junctions are present in the ridge ectoderm. Subapical mesenchyme cells show widespread expression of Cx32. (*c*) Region of the mesenchyme showing double labeling for Cx43 (*red*) and Cx32 (*green*). Note that although almost every cell expresses both connexin proteins, there is virtually no overlap between Cx32- and Cx43-containing plaques. (*d–f*) Equivalent sections through tip of mouse limb bud. Note that in the ectoderm, Cx43 (*d*) expression is restricted to the ridge itself and there is substantial expression in the mesenchyme, while Cx32 (*e*) is extremely rare in the ectoderm, although abundant in the mesenchyme. *f* shows both connexins. Again, there is no overlap between Cx43- (*red*) and Cx32- (*green*) containing gap junction plaques. (*g* and *h*) Cx32 staining by Des 5 is abolished by Des 5 peptide (*g*), but not by Gap 15 peptide (Cx43; *h*). *j* and *k* illustrate the lower Cx43 density (gap 15 antibodies) in chick posterior mesenchyme cultures maintained in the absence of FGF4 (*j*). Cx43 gap junction density is increased in posterior mesenchyme cultures maintained in FGF4 (*k*).

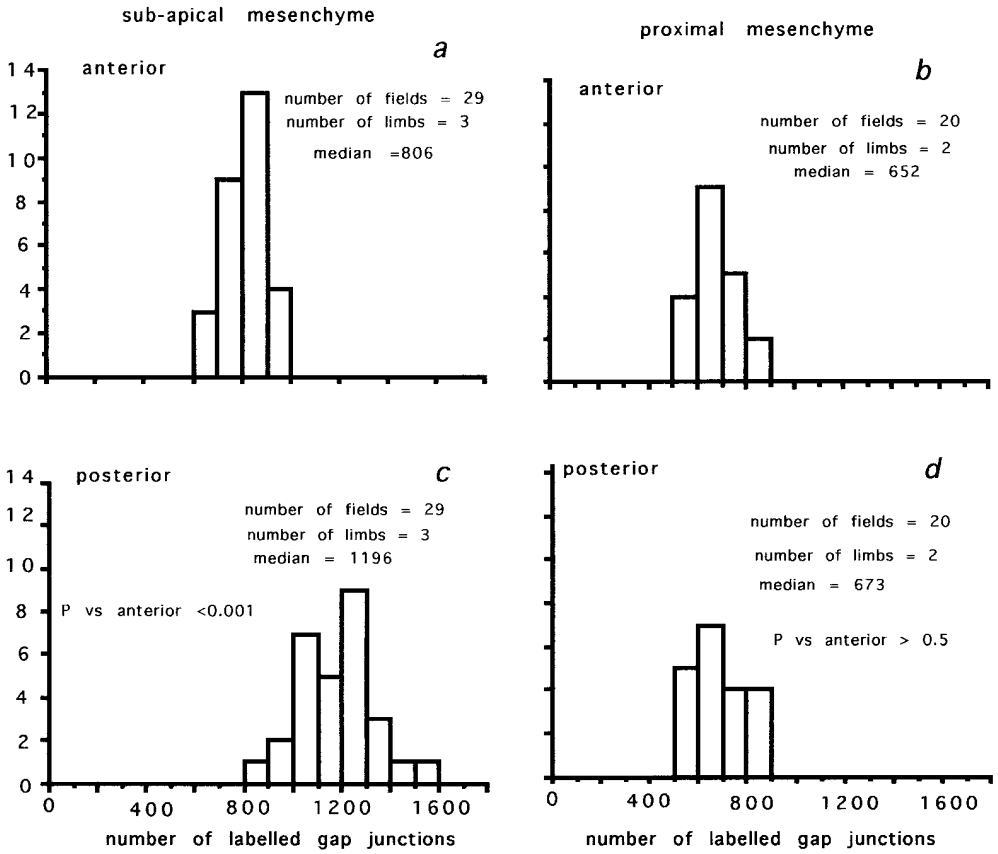

Figure 2. The density of Cx43-labeled gap junctions in the chick limb bud at HH stage 19–20. (*a* and *c*) Comparison of frequency distributions for gap junctions counted between subapical mesenchyme cells below the AER. (*a*) Anterior; (*c*) posterior. Note that the density of gap junctions is significantly ($P < 0.001$) greater between posterior mesenchyme cells, the zone of polarizing activity. (*b* and *d*) Frequency distributions for the density of gap junctions between posterior and anterior mesenchyme cells in proximal regions (150 μm back from the AER). (*b*) Anterior; (*d*) posterior. Note no difference between posterior and anterior mesenchyme.

servations. The density of Cx43-labeled gap junctions between undifferentiated chick posterior mesenchyme cells (Fig. 4, compare *b* and *d*) was more than threefold greater in cells maintained in 10 ng/ml FGF4. By contrast, anterior mesenchyme cells expressed Cx43-labeled gap junctions at the same density in the absence (Fig. 4 *a*) and presence (Fig. 4 *c*) of FGF4. In the absence of FGF4, gap junction expression between posterior mesenchyme cells (Fig. 4 *b*) was significantly lower than between anterior mesenchyme cells (Fig. 4 *a*). FGF4 did not bring Cx32 protein expression to a detectable level.

Gap junctions between undifferentiated mouse posterior and anterior mesenchyme cells showed behavior identical to chick cells (Figs. 5 [Cx43] and 6 [Cx32]). The ability of FGF4 to increase gap junction protein expression was not limited to Cx43. In mouse posterior mesenchyme cells, both Cx43- and Cx32-labeled gap junctions doubled in the presence of FGF4 (compare *b* and *d* in both figures), while gap junction density between anterior mesenchyme cells was unchanged (compare *a* and *c* in both figures and Table I). The experiment illustrated in Fig. 6 shows the only occasion on which there was any indication of FGF4 increasing gap junctions in the anterior mesenchyme (see Table I for collated results).

Results from chick mesenchyme cells plated at lower densities (2×10^4 and 1×10^4 cells/10 μl) are included in Table I, which collates results from all experiments; all possible combinations were not tested on every occasion. The relationship between gap junction density and initial plating density is not simple. However, FGF4 doubled the density of gap junctions between posterior mesenchyme cells, regardless of initial plating density. This arose from higher levels of connexin proteins in cell membranes, because cell density did not change in the presence of FGF4. At a plating density of 4×10^4 cells/10 μl, in the absence of FGF4 there were 45 ± 1.0 propidium iodide–labeled nuclei, $n = 29$, per 3,600 μm^2. When FGF4 was included there were 47 ± 1.1 nuclei, $n = 29$, per 3,600 μm^2, not significantly different ($P > 0.2$) from the density in the absence of FGF4.

The effect of FGF4 on gap junction density was restricted to undifferentiated, monolayer regions of the posterior mesenchyme. FGF4 (10 ng/ml) had no influence on gap junction density between cells in condensations. Collated results are shown in Fig. 7 for chick (Cx43: *a* and *d*) and mouse (Cx43: *b* and *e*; Cx32: *c* and *f*) posterior mesenchyme, 24 h after plating. All frequency distributions are identical. Thus, when mesenchyme cells condense, gap junction expression is maintained but is completely insensitive to FGF4.

We conclude that the expression of gap junctions between undifferentiated posterior mesenchyme cells is highly sensitive to FGF4. By contrast, anterior mesenchyme cells express the same gap junction density whether or not FGF4 is available.

FGF4 Controls Dye Transfer in Posterior Mesenchyme

The FGF4-related increase in gap junction density in posterior mesenchyme cultures was associated with a substan-

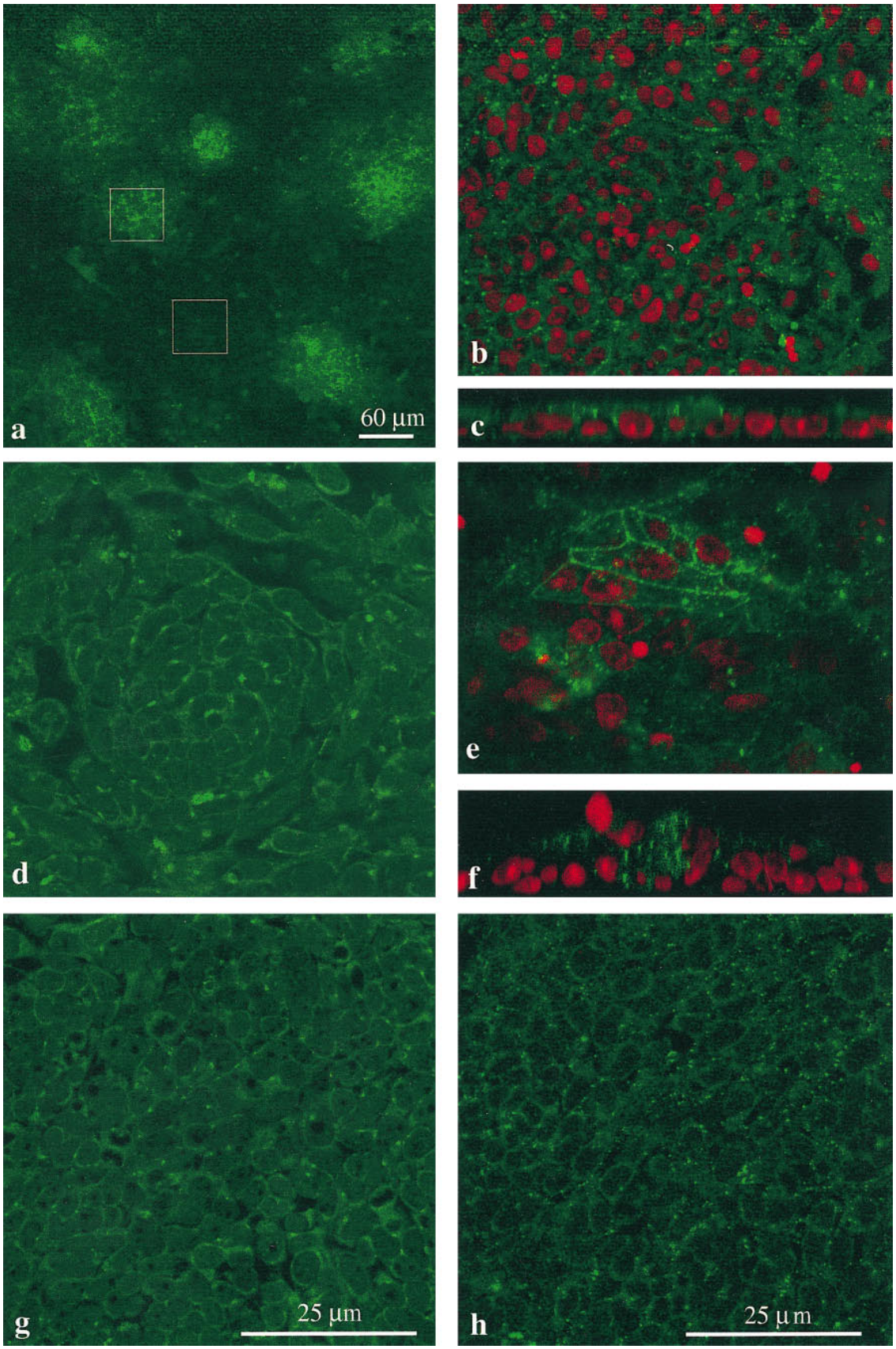

Figure 3. Connexin staining in micromass cultures. (*a–c*, *e*, and *f*) Chick mesenchyme; (*d*, *g*, and *h*) mouse mesenchyme. All images apart from *a* are at the same magnification. (*a*) Low power micrograph of chick mesenchyme culture stained for Cx43. The culture is made up of a large monolayer of undifferentiated cells interspersed with small condensations, which can be identified by the dense clustering of Cx43 staining. The box overlays show examples of regions chosen for counting. A 60 × 60–μm-sided square (3,600 μm^2) either

Table I. The Density of Gap Junctions in Control and FGF4-treated Mesenchyme Cultures

			Anterior mesenchyme: gap junctions per 3,600 μm² ± SEM *N* experiments (*n*) fields			Posterior mesenchyme: gap junctions per 3,600 μm² ± SEM *N* experiments (*n*) fields		
	Plating density	Cx	No FGF4	With FGF4	*P*	No FGF4	With FGF4	*P*
	cells/10 μl							
Chick	4×10^4		169 ± 21	155 ± 18 (a)	>0.5	164 ± 28	382 ± 53	<0.001
		43	3 (30)	3(30)		3 (26)	3 (26)	
			264 ± 24			200 ± 20		<0.02
			5 (46)			5 (42)		
	2×10^4	43				14 ± 1.1	31 ± 3	<0.007
						2 (30)	2 (30)	
	1×10^4	43				18.5 ± 1.4	28.9 ± 2.3	< 0.01
						3 (40)	3 (40)	
Mouse	4×10^4	43	378 ± 83	369 ± 82	>0.6	209 ± 22	418 ± 50	<0.001
			3 (43)	3 (43)		6 (90)	6 (80)	
		43	248 ± 16			213 ± 10		>0.1
			2 (22)			2 (22)		
		32	111 ± 17	121 ± 17	>0.8	76 ± 7	164 ± 19	<0.001
			4 (43)	4 (43)		5 (28)	5 (28)	
		32	47.6 ± 4			83.6 ± 5		<0.001
			4 (42)			4 (42)		

Results from all experiments, grouped appropriately. Data taken from single optical sections through the monolayer region of the cultures. One experiment comparing chick control and FGF4-treated anterior mesenchyme was counted as a projection and has been omitted; there was no difference ($P > 0.6$) between untreated and FGF4-treated cultures. The average number of gap junctions between cells at very low density (1×10^4) cells/10 μl) is probably overestimated because gap junctions were patchy and counts were made over regions where gap junctions could clearly be identified.

tial improvement in the efficiency of cell–cell communication. Transfer through gap junctions was assessed in chick mesenchyme cultures by injecting Lucifer yellow into one cell and counting the number of dye-containing cells. Transfer through gap junctions was taken as dye spread into more than two cells (three or more cells labeled) to eliminate any movement through bridges remaining after cytokinesis. The plating density was reduced to 1×10^4 cells/10 μl to make identification of individual cells easier. At least 10 cells were injected in each culture, without knowledge of culture conditions, and comparisons were made between treated and untreated cultures prepared in parallel.

Fig. 8 shows that functional transfer through gap junctions reflected the density of gap junctions defined by Cx protein labeling. Anterior mesenchyme cells showed the same low level of dye transfer in the absence and presence of FGF4 (compare Fig. 8, *a* and *c*; $P > 0.8$), with a failure rate (only two cells labeled) of 51% in the absence and 43% in the presence of FGF4. In the absence of FGF4, posterior mesenchyme cells transferred dye extremely poorly, with a failure rate of 60%, which is even higher than in the anterior mesenchyme (Fig. 8 *b*). By contrast, posterior mesenchyme cells in 10 ng/ml FGF4 showed greatly enhanced transfer through gap junctions (compare Fig. 8, *b* and *d*; $P < 0.0001$). Many more cells received dye, and the transfer failure rate fell to only 3%, indicating that FGF4 induced a substantial increase in functional communication. This suggests that the expanded population of gap junctions expressed in posterior mesenchyme as a result of FGF4 treatment was more permeable than the population present in either the anterior mesenchyme or the posterior mesenchyme in the absence of FGF4. Examples of dye transfer between posterior cells maintained in the absence and presence of FGF4 are shown in Fig. 8, *e* and *f*.

Signaling Capacity of Cultured Posterior Mesenchyme Cells

Unraveling the detailed cellular mechanisms that link gap junctional communication to polarizing capacity will require understanding precisely how gap junction density, functional communication, and polarizing capacity of posterior mesenchyme cells are regulated. Although previous work (Anderson et al., 1993; Vogel and Tickle, 1993) showed that culture in FGF4 improves the polarizing capacity of the posterior mesenchyme, those experiments used mouse mesenchyme cells under completely different conditions from those used here. They did not compare the polarizing capacity of cultured cells with in vivo polarizing

encloses a precartilage condensation or a region of the monolayer. (*b*) Example of region enclosed by 60-μm-sided square over an undifferentiated part of a chick mesenchyme culture stained for Cx43 (*green*) and with propidium iodide to reveal the nuclei (*red*). Spots of Cx43 label are visible around individual cells. (*c*) Image rotated through 90° to give side view shows that undifferentiated cells form a monolayer with Cx43-stained junctions between individual cells. (*e*) Example of condensation enclosed by 60-μm-sided square shows dense Cx43 labeling. (*f*) Image rotated through 90° to show cells piled up in the condensation and dense intercellular Cx43 label. (*d*) Mouse mesenchyme stained for Cx32; region containing condensation. Single optical section reveals complex cellular arrangement within the aggregate, with Cx32-containing gap junction plaques lying between individual cells. (*g*) Mouse mesenchyme: monolayer region of culture stained for Cx32. (*h*) Mouse mesenchyme: monolayer region of culture stained for Cx43.

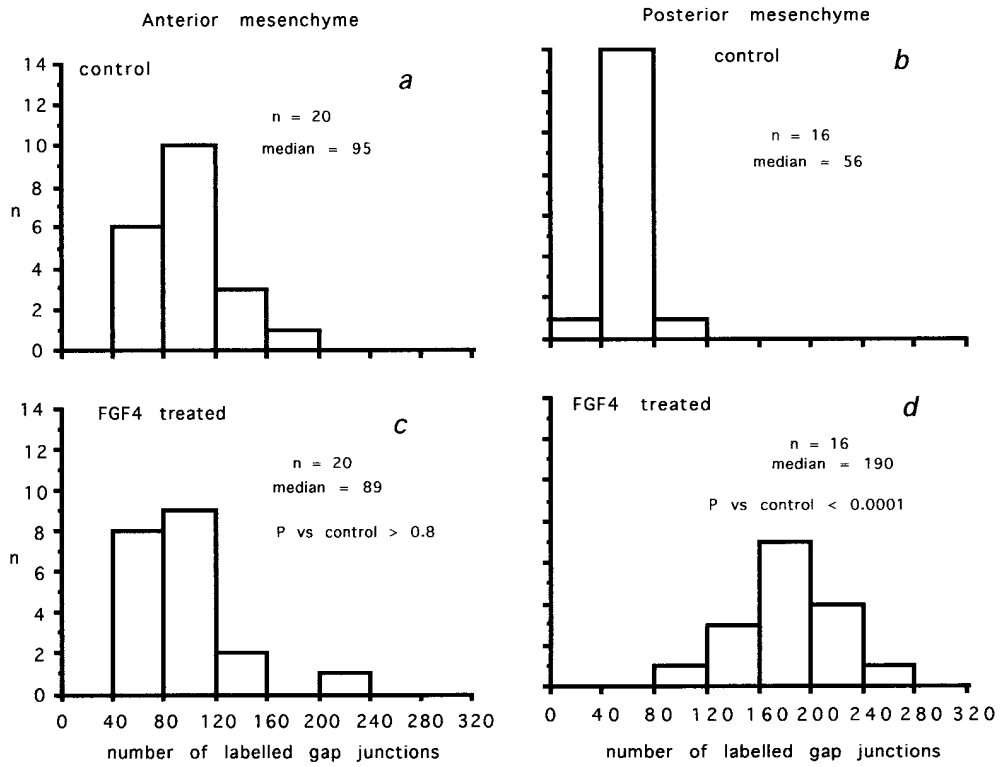

Figure 4. Chick mesenchyme: the effect of FGF4 on the density of Cx43-labeled gap junctions in monolayer regions in one of the experiments used to compile the data collated in Table I. Ordinates: number of fields. Abscissas: number of labeled gap junctions per 3,600 μm^2. (*a*) Anterior mesenchyme, no FGF4. (*b*) Posterior mesenchyme, no FGF4. (*c*) Anterior mesenchyme after culture in the presence of FGF4 for 24 h. (*d*) Posterior mesenchyme after culture in the presence of FGF4 for 24 h. Note that FGF4 markedly increases the density of gap junctions between posterior cells but has no effect on gap junctions between anterior cells.

capacity, which is derived from the ability of intact polarizing tissue grafted into host anterior mesenchyme immediately after dissection to induce limb duplications. We therefore determined the polarizing capacity of chick limb bud mesenchyme cultures maintained in the presence or absence of FGF4, plated at the densities used for analysis of gap junctions and functional communication. A small number of experiments used cells plated at 2×10^5 cells/10 μl. Signaling capacity was tested by grafting into chick hosts and expressed as the degree to which digit duplication oc-

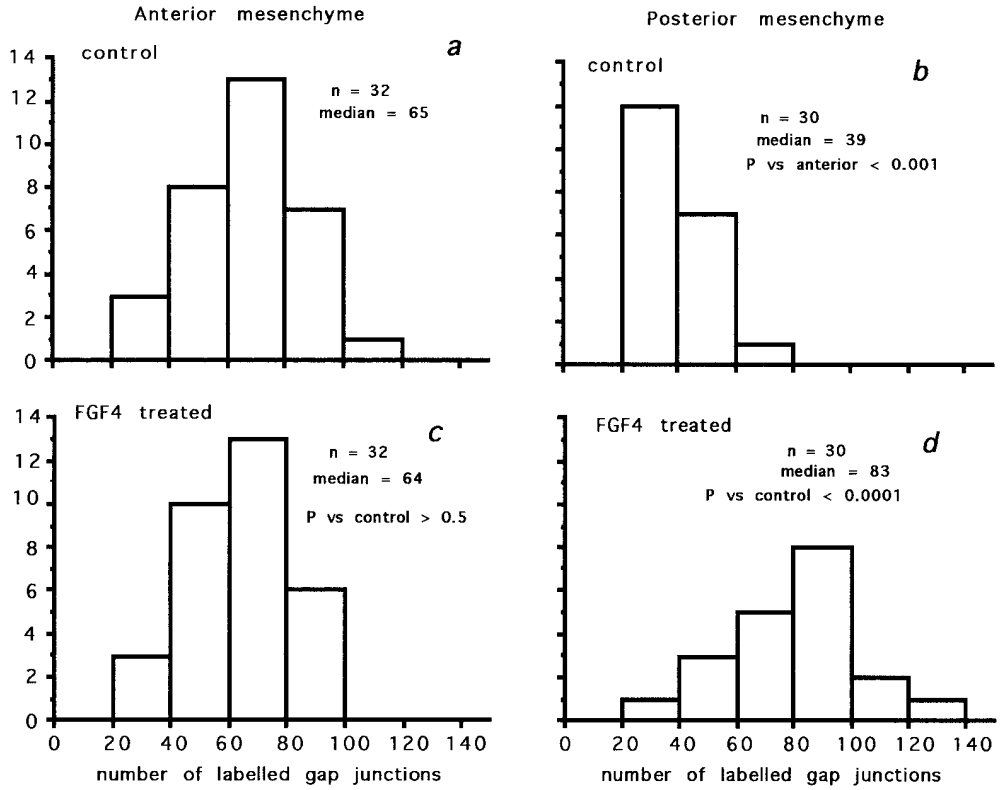

Figure 5. Mouse mesenchyme: FGF4- and Cx43-labeled gap junction in monolayer regions. Again, one experiment has been taken from the data collated in Table I. Ordinates: number of fields. Abscissas: number of labeled gap junctions per 3,600 μm^2. (*a*) Anterior mesenchyme; (*b*) posterior mesenchyme. No FGF4. (*c*) Anterior mesenchyme; (*d*) posterior mesenchyme after 24 h in FGF4. Note highly significant increase in gap junction density after treatment with FGF4.

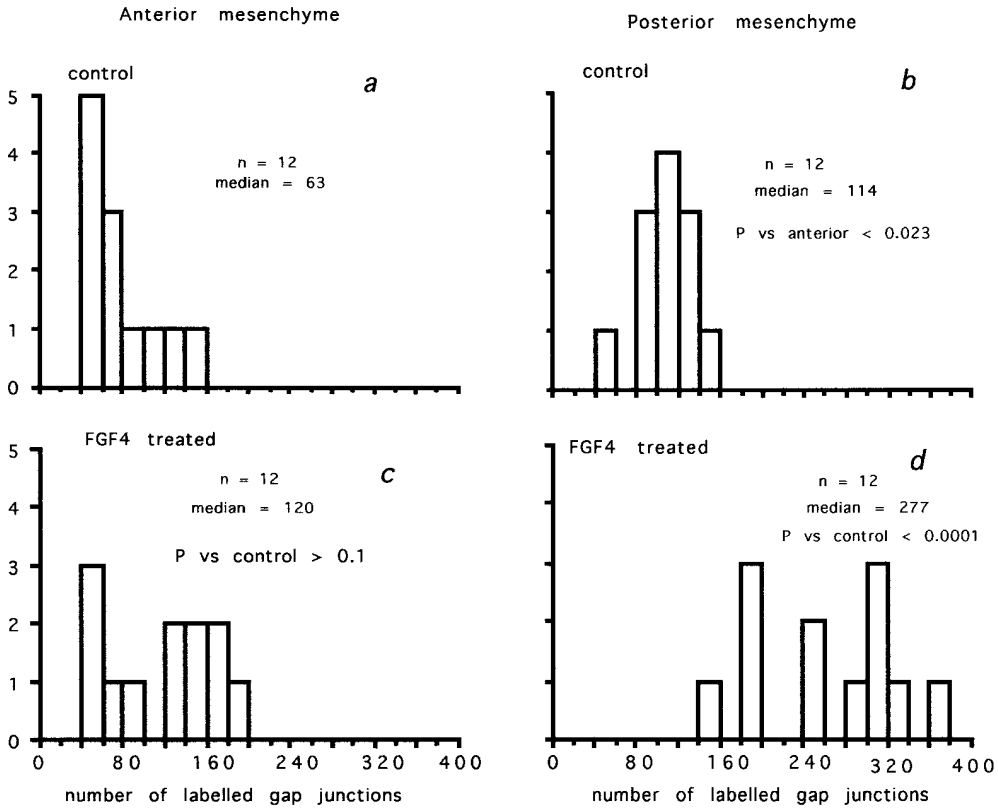

Figure 6. Mouse mesenchyme: FGF4- and Cx32-labeled gap junctions in monolayer regions; data taken from one experiment of data collated in Table I. Ordinates: number of fields. Abscissas: number of labeled gap junctions per 3,600 μm^2. (*a*) Anterior mesenchyme; (*b*) posterior mesenchyme. No FGF4. (*c*) Anterior mesenchyme; (*d*) posterior mesenchyme. FGF4. Note highly significant increase in gap junction density in posterior mesenchyme after FGF4. The small increase in gap junction density in the anterior mesenchyme observed in the presence of FGF4 was only seen in this particular experiment and was not significant.

curred (percentage respecification expressed as an average for all limb buds in each group; see Materials and Methods).

Fig. 9 *a* illustrates representative cartilage patterns observed after polarizing region grafts. Fig. 9 *b* plots percentage respecification against initial plating density for posterior mesenchyme micromasses that had been maintained for 24 h either in the absence or presence of FGF4. Per-

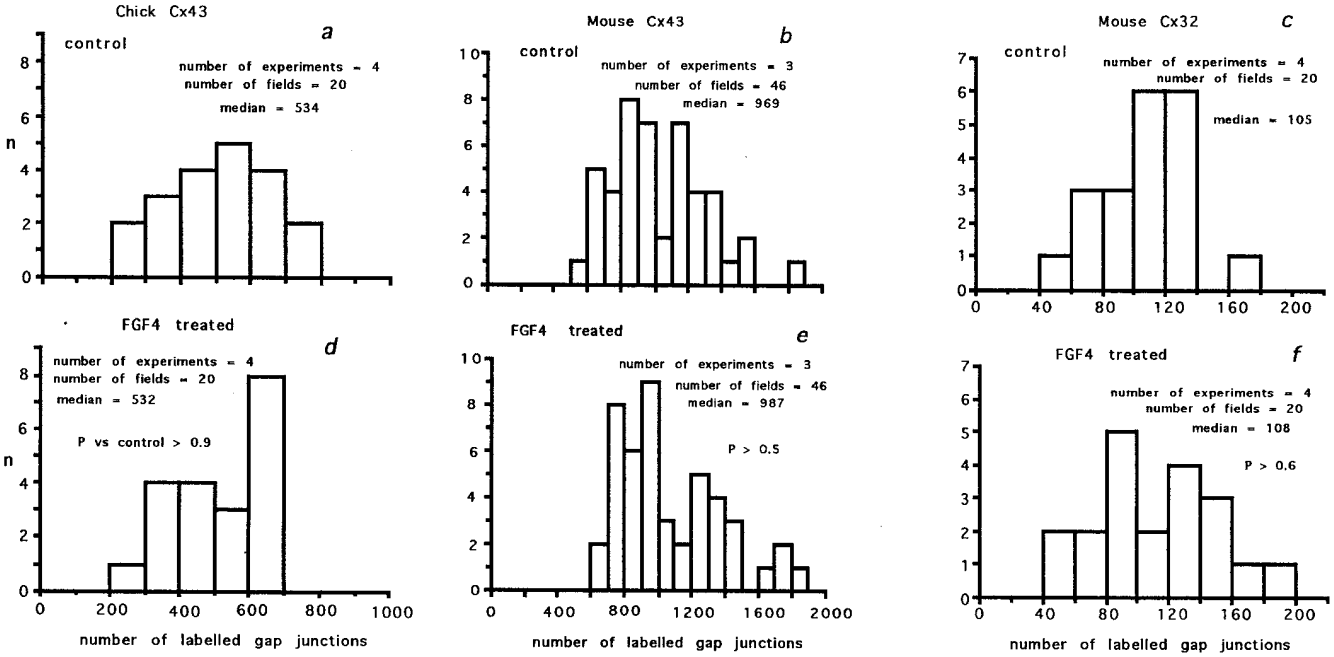

Figure 7. Connexin expression in posterior mesenchyme condensations is not sensitive to FGF4. Data summed from all experiments. Ordinates: number of fields. Abscissas: number of labeled gap junctions per 3,600 μm^2. (*a* and *d*) Chick mesenchyme Cx43. (*a*) Density of Cx43-labeled gap junctions in condensations of cultures maintained in the absence of FGF4. (*d*) Density of Cx43-labeled gap junctions in condensations of cultures maintained in the presence of FGF4. Note the frequency distributions are not significantly different ($P > 0.9$). (*b* and *e*, *c* and *f*) Equivalent plots for gap junctions in condensations in mouse mesenchyme (*b* and *e*, Cx43; *c* and *f*, Cx32). The distributions are identical whether or not FGF4 is present during culture.

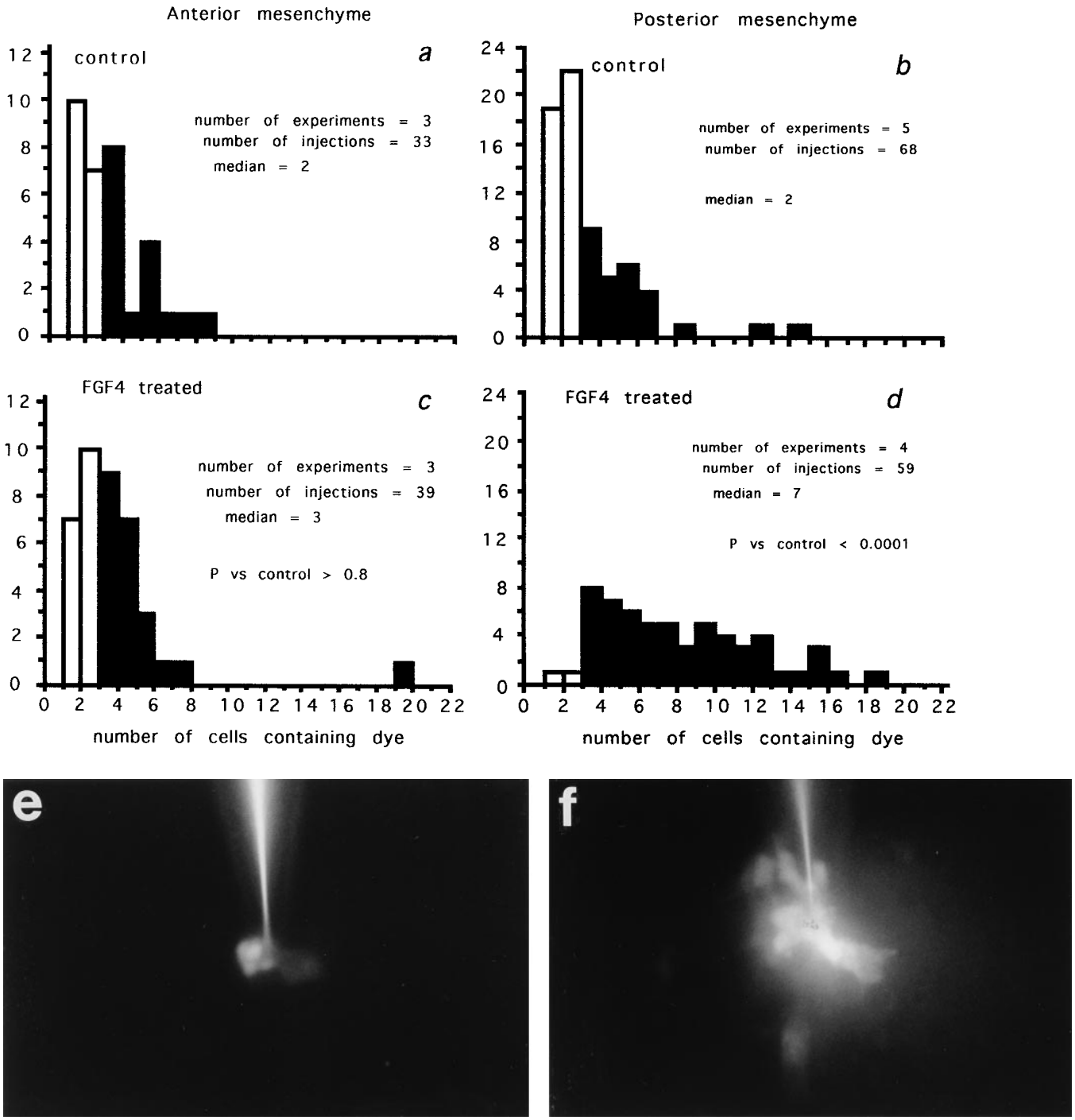

Figure 8. FGF4 increases functional transfer of Lucifer yellow through gap junctions between posterior but not anterior mesenchyme cells. In each case, the ordinate gives the number of trials, and the abscissa gives the number of cells containing Lucifer yellow after injection of Lucifer yellow into a single cell. The open columns give instances of no transfer or transfer to sister cell only, the filled columns show instances where three or more cells contained Lucifer yellow, indicating transfer through gap junctions. (*a*) Anterior mesenchyme, no FGF4. (*b*) Posterior mesenchyme, no FGF4. (*c*) Anterior mesenchyme after 24 h in FGF4. (*d*) Posterior mesenchyme after 24 h in FGF4. Note highly significant increase in instances of Lucifer yellow transfer, indicating an increased number of functional gap junctions. (*e*) Example of poor transfer in posterior mesenchyme cultured in the absence of FGF4. (*f*) Dye transfer in posterior mesenchyme maintained in FGF4. Note widespread transfer of Lucifer yellow.

centage respecification is logarithmically related to the number of cells available to respecify. In both cases, the fit is extremely good ($R > 0.99$ for both). This is shown more clearly in Fig. 9 *c*, where plating density has been plotted on a logarithmic scale. The slopes of the two relations are quite different. In the presence of FGF4, the slope was 44; the slope fell to 22 when FGF4 was not available. Without FGF4, approximately five times as many cells would be re-

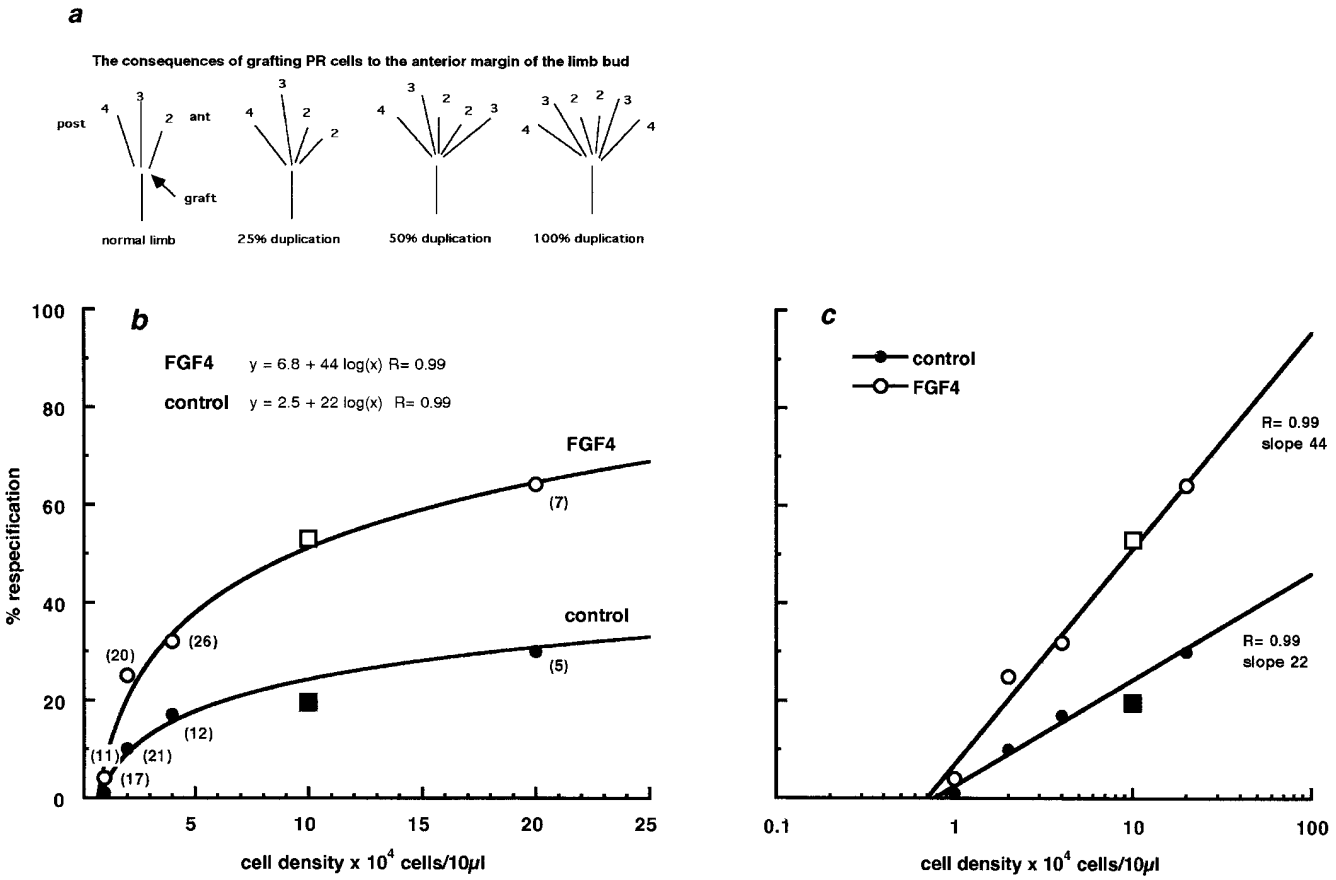

Figure 9. (*a*) Diagrams to illustrate cartilage patterns and percentage respecification observed after polarizing region grafts to the anterior margin of the chick limb bud. (*b*) Relationship between percentage respecification and cell plating density. Ordinate: percentage respecification after graft under the AER of fragment from posterior mesenchyme after 24 h in culture. Abscissa: plating density for micromass culture cells/10 μl. *Open circles*, micromasses cultured in FGF4; *filled circles*, cultures maintained in the absence of FGF4. The lines give the best logarithmic fit to the data. The figures in parentheses give the number of embryos assessed at each data point. *Squares*, data taken from Vogel and Tickle (1993) for cultures prepared from mouse polarizing cells, which fall onto the appropriate point of the logarithmic fit. (*c*) The same data plotted with the plating density on a logarithmic scale to emphasize the differences in slope of the two logarithmic fits.

quired to achieve 25% respecification (extra digit 2) and 20 times as many cells would be necessary to bring about 50% respecification (extra digit 3). Extrapolation of the plots indicates that without FGF4, the number of cells required to achieve 100% respecification (extra digit 4) increases by more than two orders of magnitude. It is extremely unlikely that a difference in the number of cells grafted could explain these observations; they suggest that cells maintained in FGF4 have a much greater polarizing capacity than cells cultured without FGF4.

How well does this relate to the high gap junction density and gap junctional communication in posterior mesenchyme maintained in FGF4? Comparison is complicated by the different methodologies used for each assay. The increase in gap junction density achieved by FGF4 was always more than twofold and was the same at each plating density, showing that the link between polarizing capacity and gap junction density cannot be linear. However, the amplification of functional communication by FGF4 was substantial and sufficient to fuel the observed improvement in polarizing capacity.

Discussion

We have shown that posterior mesenchyme cells at the tip of the limb bud, where the polarizing region is located, express significantly more gap junctions than anterior mesenchyme cells. The gradient of gap junctions from posterior to anterior is restricted to the tip of the bud and is only maintained in the presence of the AER. Parallel experiments to test the hypothesis that FGF4 controls the gradient of gap junction density across the limb bud were carried out on limb bud mesenchyme cells in micromass cultures. Gap junction expression between cells originating from the posterior mesenchyme of both the mouse and the chick limb bud was exquisitely sensitive to FGF4. By contrast, gap junctions between anterior mesenchyme cells showed no dependence on FGF4. The greater gap junction density between posterior mesenchyme cells treated with FGF4 was matched by substantially enhanced functional cell–cell communication and maintenance of the polarizing capacity of posterior mesenchyme cells at in vivo levels.

In the intact limb bud, there was a posterior–anterior gradient of both Cx43- and Cx32-containing gap junctions

at the tip of the bud, immediately beneath the AER. This strengthens the observations of Coelho and Kosher (1991), who used the scrape loading technique to assess functional communication and concluded that Lucifer yellow transfer between cells was more efficient in posterior regions of the limb bud, and Dealy et al. (1994), who found a higher level of Cx43 transcripts in posterior regions. A difference in gap junction density between posterior and anterior mesenchyme cells was no longer apparent in proximal regions. Posterior cells at the tip of the bud normally possess the greatest polarizing capacity, which declines towards proximal regions of the limb bud. Removal of the AER destroys the polarizing capacity of posterior cells. Green et al. (1994) noted that there were fewer gap junctions at the tip of the bud after removal of the AER, and we have shown that the gradient of gap junctions from posterior to anterior disappeared in the absence of the ridge. Thus, the distribution of gap junctions correlates well with polarizing capacity.

Once mesenchyme cells leave the progress zone of the limb bud, posterior cells no longer possess polarizing capacity, and their positional values are fixed before differentiation. The posterior–anterior gap junction gradient disappeared in proximal regions. A parallel may be drawn with the aggregates of condensed cells in cultures, some of which will go on to form cartilage nodules. In both chick and mouse posterior mesenchyme, once cells had condensed, the density of gap junctions was no longer sensitive to FGF4. This suggests that growth factor sensitivity and the functional role of gap junctions may change in preparation for differentiation.

What mechanism underlies the gradient of gap junctions at the tip of the limb bud? *Fgf4* transcript expression is localized to the posterior ectoderm ridge, and a straightforward hypothesis would be that secretion of FGF4 by posterior ridge cells controls the expression of gap junctions in the mesenchyme. We tested this hypothesis by determining whether gap junctions between mesenchyme cells are sensitive to FGF4. Mesenchyme cells in culture were used, which allowed the sensitivity of gap junctions to FGF4 to be tested directly. The results were both unequivocal and somewhat unexpected. Both in chick and mouse posterior mesenchyme, the density of gap junctions, whether constructed from Cx43 or Cx32, was highly significantly increased when undifferentiated posterior mesenchyme cells, which emit signals that can respecify anterior mesenchyme, were cultured in the presence of FGF4. Functional communication between posterior mesenchyme cells, assessed by dye transfer, also was substantially increased when FGF4 was present. This response was restricted to the posterior mesenchyme. In anterior mesenchyme cells, neither gap junction density nor functional communication was affected by FGF4. Both Cx43- and Cx32-containing gap junctions behaved identically, showing that the influence of FGF4 on mesenchyme cells is not connexin specific. The results provide strong evidence for the hypothesis that high gap junction density and functional communication in the posterior subapical mesenchyme of the intact limb bud stem from the localized expression of *Fgf4* transcripts in the posterior ridge. The insensitivity of gap junctions between anterior mesenchyme cells to FGF4 leads to the conclusion that in the anterior mesenchyme, any effects of FGF4 that form part of the response to a polarizing signal are not mediated by alterations in gap junction density or functional communication through gap junctions. The possibility that other FGFs may act through gap junctions to maintain the responsiveness of anterior mesenchyme cells remains open.

How do these results fit with evidence emerging from "knockout" mice? Knockouts for both Cx43 (Reaume et al., 1995) and Cx32 (Nelles et al., 1996) have now been described. Gross defects in the limb buds are not apparent, which indicates that either Cx43 or Cx32 is sufficient to sustain the contribution of gap junctions to limb bud patterning. This fits our observation that both Cx43- and Cx32-containing gap junctions between posterior mesenchyme cells are sensitive to FGF4. Clearly the outcome of a double Cx43/Cx32 knockout will be very interesting, although even there the possibility that other connexins may come into play remains open.

The posterior mesenchyme at the tip of the limb bud includes polarizing cells with the capacity to respecify anterior mesenchyme when grafted into the anterior margin of a host limb bud. If the differential effects of FGF4 on gap junctions in posterior and anterior mesenchyme are linked to polarizing capacity, then posterior cells whose gap junctions are sensitive to FGF4 should possess greater polarizing capacity when FGF4 is available. This prediction was amply substantiated. The slope of the relationship between cell density and percentage respecification (see Fig. 9 *c*) should remain the same so long as signaling ability does not alter; an increase or decrease in the absolute number of polarizing cells will simply shift the plot along the abscissa. When plotted in the same way as the present results in Fig. 9 *c*, Allen et al.'s (1990) control results give a slope of 42 ($R = 0.96$), while Tickle's (1981) results give a slope of 40 ($R = 0.93$). In both these cases, cells were grafted as pellets shortly after removal from donor limb buds and represent normal polarizing capacity. For posterior mesenchyme cultures maintained for 24 h in FGF4, the slope was very similar at 44 ($R = 0.99$). This leads to an important new conclusion: When polarizing region cells are cultured in FGF4 for 24 h, their capacity to polarize is maintained at the in vivo level, which is associated with the retention of gap junctions that are controlled by FGF4. If withdrawing FGF4 were to reduce the number of polarizing cells without altering the effectiveness with which each individual cell signals, the relationship between percentage respecification and cell density should simply shift to higher cell densities; there would be no change in slope. However, for posterior mesenchyme cells maintained in the absence of FGF4, the logarithmic slope halved from 44 to 22 (see Fig. 9 and accompanying text). Withdrawal of FGF4 not only leads to the loss of FGF4-sensitive gap junctions but also alters the signaling mechanism. The ability to separate differences in polarizing capacity that derive from changes in the number of signaling cells from those that derive from an alteration in signaling mechanism will assist the mechanistic analysis of limb bud patterning.

Cells that express the FGF4-sensitive gap junction population share some important properties with *Shh*-expressing cells. Gap junction regulation in response to FGF4 is restricted to posterior mesenchyme cells; gap junctions be-

tween anterior mesenchyme cells do not respond by increasing gap junction density or functional communication, although there may be other effects on gap junction properties. Similarly, FGF4 maintains *Shh* expression, which has been shown to generate a polarizing signal, in the posterior mesenchyme; FGF4 cannot switch on *Shh* expression in anterior mesenchyme cells. The posterior–anterior gradient of gap junctions between cells disappears in proximal regions of the bud where no *Shh* expression is found. Are gap junctional communication and *Shh* expression in posterior mesenchyme cells controlled by FGF4 independently, in parallel, or sequentially? One possibility is that FGF4-sensitive gap junctional communication between polarizing cells regulates *Shh* levels to modulate the stimulatory effects of FGF4. There is evidence to support this suggestion. Polarizing cells plated as dispersed individuals onto plastic film appear more effective at respecifying the limb bud than polarizing cells grafted with anterior mesenchyme as mixed pellets (Tickle, 1981). Polarizing cells loaded with antibodies that block cell–cell communication (Allen et al., 1990) and grafted as a mixed posterior–anterior mesenchyme cell pellet not only retain but may increase (see Allen, 1988) polarizing activity. It is worth noting that FGF/*Shh* interactions (Bueno et al., 1996) are a feature of a number of developing systems in which cells are linked by gap junctions. The present results may, therefore, have wide applicability.

Our results lend strong support to the hypothesis that growth factor signaling and gap junctional communication are coordinately regulated in the limb bud and that this is an integral part of the regulation of polarizing capacity in posterior mesenchyme cells. The similarity between the control exerted by FGF4 on gap junction density and functional communication and *Shh* expression opens up new avenues for exploration of cellular mechanisms in the limb bud. It should now be possible to begin the more difficult task of integrating the regulation of other genes that encode potentially important signaling molecules into detailed cellular mechanisms that underlie limb bud patterning.

We thank John Heath for a gift of FGF4.

This work was supported by the Wellcome Trust International Travelling Fellowship to H. Makarenkova (grant No. 042268; confocal grant 040738/Z/94/A). David Becker and Anne Warner thank the Royal Society for their support.

Received for publication 17 December 1996 and in revised form 27 June 1997.

References

Allen, F.L.G. 1988. Gap junctional communication during patterning of the limb and neuromuscular junction formation. PhD thesis. University of London, London, UK.

Allen, F.L.G., C. Tickle, and A. Warner. 1990. The role of gap junctions in patterning of the chick limb bud. *Development (Camb.).* 108:623–634.

Anderson, R., M. Landry, and K. Muneoka. 1993. Maintenance of ZPA signalling in cultured mouse limb bud cells. *Development (Camb.).* 117:1421–1433.

Becker, D.L., W.H. Evans, C.R. Green, and A.E. Warner. 1995. Functional analysis of amino acid sequences in connexin43 involved in intercellular communication through gap junctions. *J. Cell Sci.* 108:1455–1467.

Bueno, D., J. Skinner, H. Abud, and J.K. Heath. 1996. Spatial and temporal relationships between *shh*, *Fgf-4* and *Fgf-8* gene expression at diverse signalling centers during mouse development. *Dev. Dyn.* 207:291–299.

Coelho, C.N., and R.A. Kosher. 1991. A gradient of gap junctional communication along the anterior-posterior axis of the developing chick limb bud. *Dev. Biol.* 148:529–535.

Dealy, C.N., E.C. Beyer, and R.A. Kosher. 1994. Expression patterns of mRNAs for gap junction proteins, connexin43 and connexin42 suggest their involvement in chick limb morphogenesis and specification of the arterial vasculature. *Dev. Dyn.* 199:156–167.

Fallon, J.F., A. López, M.A. Roz, M.P. Savage, B.B. Olwin, and B.K. Simandl. 1994. FGF2: apical ectodermal ridge growth signal for chick limb development. *Science (Wash. DC).* 264:104–107.

Green, C.R., N.S. Peters, R.G. Gourdie, S. Rothery, and N.J. Severs. 1993. Validation of immunohistochemical quantification in confocal laser scanning microscopy: a comparative assessment of gap junction size with confocal and ultrastructural techniques. *J. Histochem. Cytochem.* 41:1339–1349.

Green, C.R., L. Bowles, A. Crawley, and C. Tickle. 1994. Expression of the connexin43 gap junctional protein in tissues at the tip of the chick limb bud is related to the epithelial-mesenchymal interactions that mediate morphogenesis. *Dev. Biol.* 161:12–21.

Laird, D.W., S.B. Yancey, L. Bugga, and J.-P. Revel. 1992. Connexin expression and gap junction communication compartments in the developing mouse limb. *Dev. Dyn.* 195:153–161.

Laufer, E., C.E. Nelson, R.L. Johnson, B.A. Morgan, and C. Tabin. 1994. Sonic hedgehog and FgF-4 act through a signalling cascade and feedback loop to integrate growth and patterning of the developing limb bud. *Cell.* 79:993–1003.

Nelles, E., C. Butzler, D. Jung, A. Temme, H.D. Gabriel, U. Dahl, O. Traub, F. Stumpel, K. Jungermann, J. Zielasek, et al. 1996. Defective propagation of signals generated by sympathetic nerve stimulation in the liver of connexin32-deficient mice. *Proc. Natl. Acad. Sci. USA.* 93:9565–9570.

Niswander, L., C. Tickle, A. Vogel, I. Booth, and G.R. Martin. 1993. FGF-4 replaces the apical ectodermal ridge and directs outgrowth and patterning of the limb. *Cell.* 75:579–587.

Niswander, L., S. Jeffrey, G.R. Martin, and C. Tickle. 1994. A positive feedback loop coordinates growth and patterning in the vertebrate limb. *Nature (Lond.).* 371:609–612.

Reaume, A.G., P.A. de Sousa., S. Kulkarni, B.L. Langille, D. Zhu, T.C. Davies, S.C. Juneja, G.M. Kidder, and J. Rossant. 1995. Cardiac malformation in neonatal mice lacking connexin43. *Science (Wash. DC).* 267:1831–1834.

Riddle, R.D., R.L. Johnson, E. Laufer, and C. Tabin. 1993. Sonic hedgehog mediates the polarising activity of the ZPA. *Cell.* 75:1402–1416.

Saunders, J.W. 1948. The proximo-distal sequence of origin of limb parts of the chick wing and the role of the ectoderm. *J. Exp. Zool.* 108:363–404.

Saunders, J.W., and M.T. Gasseling. 1968. Ectodermal-mesodermal interactions in the origin of limb symmetry. *In* Epithelial-Mesenchymal Interactions. R. Fleischmajer and R.E. Billingham, editors. Williams and Wilkins, Baltimore. 78–97.

Summerbell, D. 1974. A quantitative analysis of the effect of excision of the AER from the chick limb bud. *J. Embryol. Exp. Morphol.* 35:241–260.

Tickle, C. 1981. The number of polarising region cells required to specify additional digits in the developing chick wing. *Nature (Lond.).* 289:295–298.

Tickle, C., G. Shellswell, A. Crawley, and L. Wolpert. 1976. Positional signalling by mouse limb polarising region in the chick limb bud. *Nature (Lond.).* 259:396–397.

Vogel, A., and C. Tickle. 1993. FGF-4 maintains polarising activity of posterior limb bud cells in vivo and in vitro. *Development (Camb.).* 119:199–206.